JOURNAL OF SPACECRAFT AND ROCKETS
Vol. 40, No. 3, May–June 2003

Engineering Notes

ENGINEERING NOTES are short manuscripts describing new developments or important results of a preliminary nature. These Notes cannot exceed six manuscript pages and three figures; a page of text may be substituted for a figure and vice versa. After informal review by the editors, they may be published within a few months of the date of receipt. Style requirements are the same as for regular contributions (see inside back cover).

Transfer Between Circular and Hyperbolic Orbits Using Analytical Maximum Thrust Arcs

Dilmurat M. Azimov* and Robert H. Bishop†
University of Texas at Austin, Austin, Texas 78712

Introduction

IT is known that in the case of motion in a central Newtonian field there may exist two different types of optimal trajectory structure. The first trajectory structure contains null thrust (NT), intermediate thrust, and maximum thrust (MT) arcs[1] and consists of null and maximum power arcs.[2] It has been shown that, in the case of constraints on unit thrust direction cosines, specific impulse, and power, one can obtain analytical trajectories associated with constant or variable exhaust speed.[3] In this Note, the same problem statement used to describe the low thrust (LT) arcs[3] is used to obtain analytic MT arcs and to investigate the transfer between circular and hyperbolic orbits in a Newtonian gravity field. This represents a step toward a generalized problem statement from which many optimal space trajectory analytic solutions flow and from which existing thrust arcs can be classified.

The equations of optimal motion can be represented as a 14th-order canonical system of equations, and the principal difficulty of solving the problem in quadratures for the MT arcs consists of finding two first integrals of this canonical system.[4] However, an analytical approximation of the Newtonian gravity field by a linear central field during the motion on an MT arc leads to closed-form analytical solutions.[5] Investigations of MT arcs obtained by various numerical and approximate analytical methods may be found in Refs. 6–12. In the present Note, it will be shown that the linear field approximation can be used to analyze the maximum thrust transfer maneuver mentioned earlier.

Variational Problem Statement

Consider a spacecraft with mass m, the motion of which is described by the continuous vector functions position $\boldsymbol{r}$ and velocity $\boldsymbol{v}$. The spacecraft is equipped by a propulsion system with exhaust velocity c, exhaust power $P\,(P \le P_{\max})$, and specific impulse I_{sp}, where $I_{\mathrm{sp}_{\min}} \le I_{\mathrm{sp}} \le I_{\mathrm{sp}_{\max}}$. The equations of motion can be given as[3]

$$\dot{\boldsymbol{x}} = \boldsymbol{f}(\boldsymbol{x}, \boldsymbol{u}) \tag{1}$$

with

$$\boldsymbol{x} = \begin{bmatrix} \boldsymbol{r} \\ \boldsymbol{v} \\ m \end{bmatrix}$$

$$\boldsymbol{f}(\boldsymbol{x}, \boldsymbol{u}) = \begin{bmatrix} \boldsymbol{v} \\ -\dfrac{\mu}{r^3}\boldsymbol{r} + \dfrac{2P}{I_{\mathrm{sp}} g m}\boldsymbol{l} \\ -\dfrac{2P}{I_{\mathrm{sp}}^2 g^2} \end{bmatrix}, \qquad \boldsymbol{u} = \begin{bmatrix} \boldsymbol{l} \\ P \\ I_{\mathrm{sp}} \end{bmatrix}$$

where $\boldsymbol{l} = [l_1, l_2, l_3]^T$ is the piecewise continuous unit thrust vector, $\boldsymbol{u}$ is the control input vector, μ is the gravitational parameter of the central body, and g is the sea-level gravitational acceleration. The objective is to transfer the spacecraft from the initial state $\boldsymbol{r}_0$, $\boldsymbol{v}_0$, and m_0 at t_0 to the final state $\boldsymbol{r}_1$, $\boldsymbol{v}_1$, and m_1 at t_1, while minimizing the performance index,

$$\mathcal{J} = m_0 - m_1 \tag{2}$$

subject to the control constraints

$$h_1 := l_1^2 + l_2^2 + l_3^2 - 1 = 0, \qquad h_2 := P(P_{\max} - P) - \gamma^2 = 0$$
$$h_3 := \left(I_{\mathrm{sp}_{\max}} - I_{\mathrm{sp}}\right)\left(I_{\mathrm{sp}} - I_{\mathrm{sp}_{\min}}\right) - \eta^2 = 0 \tag{3}$$

where η and γ are additional control variables and, consequently, $\boldsymbol{u} = [\boldsymbol{l}^T \;\; P \;\; I_{\mathrm{sp}} \;\; \eta \;\; \gamma]^T$. The flight time is assumed to be arbitrary.

In the analysis of the trajectories associated with chemical propulsion systems, we attempt to minimize the equivalent free space velocity:

$$\int a_t(t)\,\mathrm{d}t$$

that is, the speed that the spacecraft would reach in the absence of gravitational and drag forces. The magnitude of the acceleration due to thrust is denoted by a_t. In the case of power-limited propulsion systems, the performance index

$$\int a_t^2(t)\,\mathrm{d}t$$

is considered to maximize the final mass (payload). For these integrals, we have

$$\frac{1}{m_1} = \frac{1}{m_0} + \int_{t_0}^{t_1} \frac{a_t^2(t)}{2P(t)}\,\mathrm{d}t$$

Similarly,

$$\mathcal{J} = \int_{t_0}^{t_1} a_t(t)\,\mathrm{d}t = c\,\ell n\frac{m_0}{m_1} \tag{4}$$

the minimization of which is equivalent to minimization of $\mathcal{J}$ in Eq. (2) (Ref. 10). If $P = P_{\max}$, from the preceding expressions it follows that the minimization of the integral

$$\int a_t^2\,\mathrm{d}t$$

Presented as Paper AAS 02-155 at the AAS/AIAA 12th Space Flight Mechanics Meeting, San Antonio, TX, 27–31 January 2002; received 22 September 2002; revision received 3 November 2002; accepted for publication 15 February 2003. Copyright © 2003 by Dilmurat M. Azimov and Robert H. Bishop. Published by the American Institute of Aeronautics and Astronautics, Inc., with permission. Copies of this paper may be made for personal or internal use, on condition that the copier pay the $10.00 per-copy fee to the Copyright Clearance Center, Inc., 222 Rosewood Drive, Danvers, MA 01923; include the code 0022-4650/03 $10.00 in correspondence with the CCC.

*Research Engineer/Scientist Associate, Department of Aerospace Engineering and Engineering Mechanics; azimov@csr.utexas.edu. Member AIAA.

†Professor, Department of Aerospace Engineering and Engineering Mechanics; rhbishop@mail.utexas.edu. Associate Fellow AIAA.

is equivalent to the minimization of the integral

$$\int a_t \, \mathrm{d}t$$

Consequently, it can be concluded that both the LT and HT arcs can be considered under one problem statement.

Analytical Solutions for Maximum Thrust Arcs

When the linear approximation of a central Newtonian field is considered, the second-order differential equations for the radius vector and primer vector can be written as

$$\ddot{\boldsymbol{r}} + \left(\mu/r_0^3\right)\boldsymbol{r} = \boldsymbol{a}_t, \qquad \ddot{\boldsymbol{\lambda}} = -\left(\mu/r_0^3\right)\boldsymbol{\lambda} \tag{5}$$

An analysis of these equations indicates that the linear approximation is admissible if $\sin\varphi \approx 0$ and $\Delta r/r_0 \ll 1$.

The detailed analysis of Eq. (5) presented in Ref. 5 is not repeated here; however, the obtained analytical solutions are given next for completeness. In the case of free final time, the analytical solutions for the MT arcs include, in particular, the following expressions:

$$v_1 = r[k\cot(kt+\alpha) + \dot{\varphi}\tan\varphi]$$

$$v_2 = -aC_2k\frac{\sin\varphi}{\cos(kt+\alpha)} + \frac{\chi\beta}{ak}\frac{2\cos^2\varphi}{aC_2\sin 2(kt+\alpha)}$$

$$r = aC_2\frac{\sin(kt+\alpha)}{\cos\varphi}, \qquad \theta = \varphi + \psi_0 - \frac{\pi}{2}, \qquad m = m_0 - \beta t$$

$$\lambda_1 = a\sin(kt+\alpha)\sin\varphi, \qquad \lambda_2 = a\sin(kt+\alpha)\cos\varphi$$

$$\psi = \psi_0 = \text{const} \tag{6}$$

where

$$\tan\varphi = \frac{\tan\alpha\tan\varphi_0}{\tan(kt+\alpha)} + \frac{\chi\beta}{ak}\frac{1}{aC_2k} + \frac{cs}{aC_2k\tan(kt+\alpha)}$$

$$\chi = -\frac{akc}{\beta}[F_1(x_0,x)\sin(\alpha_0) + F_2(x_0,x)\cos(\alpha_0)]$$

$$s = F_2\sin\alpha_0 - F_1\cos\alpha_0, \qquad F_1 := F_1(x_0,x) = Si(x) - Si(x_0)$$

$$F_2 := F_2(x_0,x) = Ci(x) - Ci(x_0)$$

$$x := \frac{km_0}{\beta} - kt, \qquad x_0 := \frac{km_0}{\beta}, \qquad \alpha_0 := \alpha + \frac{km_0}{\beta}$$

and the functions $Si(x)$ and $Ci(x)$ are integral sine and integral cosine functions, φ is the thrust angle, and φ_0, α, a, m_0, ψ_0, and λ_{70} are integration constants.[5]

Transfer Between Circular and Hyperbolic Orbits via MT Arc

It is well known that the minimum fuel transfer between given circular and hyperbolic orbits in the Newtonian field can be implemented by instantaneous velocity change, which means application of an impulse on the pericenter of the hyperbolic orbit, assuming that $\beta \to \infty$ (Ref. 1). In this section, it will be shown that this transfer can be implemented by using an MT arc described by the closed-form analytical solution given in the preceding section. It is assumed that 1) the gravitational acceleration on the MT arc is a linear function of the radius vector and 2) the hyperbolic orbit is tangent to the initial circular orbit at its perigee. The manuever geometry is shown in Fig. 1. The trajectory with the structure NT–MT–NT, where the NT arcs represent the terminal orbits, is considered. The transfer trajectory contains two switching points, located on the terminal orbits. The functional is chosen to be $\mathcal{J} = m_0 - m_1$. At $t = t_1 = 0$, the initial conditions are $r = r_0$, $v_{11} = 0$, $v_{21} = kr_0$, and $m = m_0$, and at the final time, $t = t_2$, the conditions are $\boldsymbol{r}(p, e, f_2)$ and $\boldsymbol{v}(p, e, f_2)$, where f_2 is to be determined. At any point of the optimal trajectory, the radius, velocity, and primer vectors must all be continuous, and

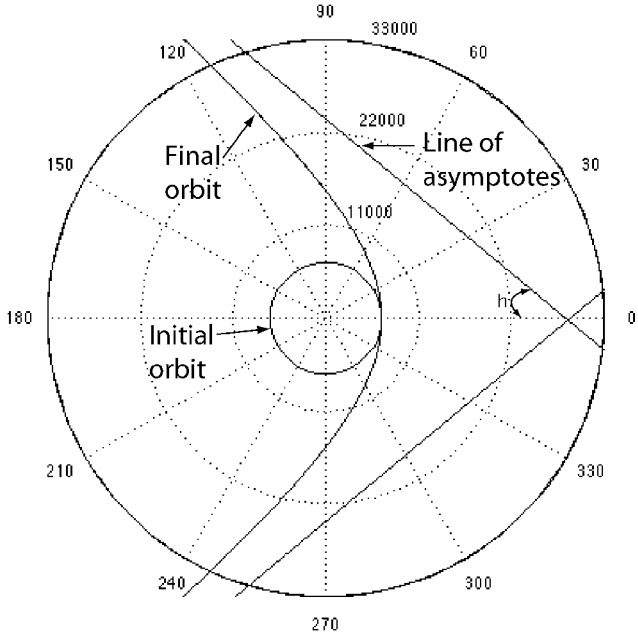

Fig. 1 Maneuver geometry.

the switching function[1] $\chi = 0$. The continuity conditions at the first switching point are

$$0 = \varphi_1 + \psi_1 - \pi/2, \qquad r_0 = aC_2(\sin\alpha/\cos\varphi_1)$$

$$kr_0 = aC_2(\sin\alpha/\cos\varphi_1)\dot{\varphi}_1, \qquad \dot{\varphi}_1 = -k\sin 2\varphi_1/\sin 2\alpha$$

$$P_1\sin f_1 = a\sin\alpha\sin\varphi_1, \qquad 2P_1\cos f_1 + R_1 = a\sin\alpha\cos\varphi_1$$

The conditions at the second switching point are

$$F_1\sin\alpha_1 + F_2\cos\alpha_1 = 0$$

$$\theta_2 = \varphi_2 + \psi_2 - \frac{\pi}{2} = f_2 + \omega \tag{7}$$

$$\frac{p}{1+e\cos f_2} = aC_2\frac{\sin(kt_2+\alpha)}{\cos\varphi_2} \tag{8}$$

$$\sqrt{\frac{\mu}{p}}e\sin f_2 = aC_2\frac{\sin(kt+\alpha)}{\cos\varphi_2}[k\cot(kt+\alpha) + \dot{\varphi}_2\tan\varphi_2] \tag{9}$$

$$\sqrt{\frac{\mu}{p}}(1+e\cos f_2) = aC_2\frac{\sin(kt_2+\alpha)}{\cos\varphi_2}\dot{\varphi}_2 \tag{10}$$

$$P_2e\sin f_2 = a\sin(kt_2+\alpha)\sin\varphi_2$$

$$P_2(1+e\cos f_2) + \frac{R_2}{1+e\cos f_2} = a\sin(kt_2+\alpha)\cos\varphi_2$$

where f_1 and f_2 are the true anomalies, $\theta_1 = 0$ is the polar angle of the initial point of the MT arc,

$$\tan\varphi_2 = \frac{\tan\varphi_1\tan\alpha}{\tan(kt_2+\alpha)} + \frac{cs}{aC_2k\tan(kt_2+\alpha)}$$

$$\dot{\varphi}_2 = -\frac{k\sin 2\varphi_2}{\sin 2(kt_2+\alpha)}, \qquad s = F_2\sin\alpha_1 - F_1\cos\alpha_1$$

$$\alpha_1 = \alpha + \frac{km_0}{\beta}, \qquad x_1 = \frac{km_0}{\beta}, \qquad x_2 = \frac{km_0}{\beta} - kt_2$$

$$F_1 = Si(x_2) - Si(x_1), \qquad F_2 = Ci(x_2) - Ci(x_1),$$

where p, e, and ω are parameters of the elliptic transfer orbit, t_1 and t_2 are the initial and final times on the MT arc, respectively, and

Table 1 Parameter solutions at the two switching points

Switching point	t	r	θ	v_1	v_2	m	φ	ψ
First	0	6600	0	0	7.7714	10000	−0.05285	1.6236
Second	110.69	6611.2	0.15661	0.51383	11.766	2620.9	0.05157	1.6236

$\psi_2 = \psi_1$ because ψ is a constant. P_1, P_2, R_1, and R_2 are known as Lawden's integration constants.[1]

From the transversality condition and condition $\chi(t_2) = 0$, we obtain

$$\lambda_{71} = -\frac{\partial \mathcal{J}}{\partial m_1} = 1, \qquad ca\sin(kt_2 + \alpha) = m_0 - \beta t_2 \tag{11}$$

From the conditions at the first switching point it can be shown that

$$\alpha_1 = \arctan(-F_2/F_1) - km_0/\beta, \qquad \alpha = \alpha_1 - km_0/\beta$$

$$f_1 = \arctan(-\sin 2\alpha_1/2)$$

$$\varphi_1 = \alpha + \pi/2, \qquad \dot{\varphi}_1 = k, \qquad r_0 = -C_2 a_1 \tag{12}$$

and from the conditions at the second switching point, we obtain

$$\tan\varphi_2 \tan(kt_2 + \alpha) = -(1 + cs/kr_0) \tag{13}$$

Substituting the integration constant from Eq. (12) into Eq. (8) for the radius vector magnitude yields

$$1 + e\cos f_2 = -(p/r_0)(\cos\varphi_2/\sin\gamma)$$

where $\gamma = kt_2 + \alpha$. Consequently, from Eq. (10) it follows that

$$\tan^2\varphi_2 \tan^2\gamma = p/r_0, \qquad p/r_0 = (1 + cs/kr_0)^2 \tag{14}$$

At given p, r_0, c, m_0, and β, Eq. (14) can be used to find the final time t_2. From Eqs. (9) and (10), it can be found that

$$e\sin f_2 = -\sqrt{\frac{p}{r_0}}\left(\frac{\cos^2\gamma - \sin^2\varphi_2}{\cos\gamma\cos\varphi_2}\right)$$

$$e\cos f_2 = -\sqrt{\frac{p}{r_0}}\frac{\sin\varphi_2}{\cos\gamma} - 1$$

from which, by denoting the first equation by e_1 and the second equation by e_2, one can obtain

$$\tan f_2 = e_1/e_2, \qquad e^2 = e_1^2 + e_2^2$$

Consequently, the unknowns at the second switching point, r_2, v_1, v_2, θ_2, and φ_2 can be computed based on Eqs. (7), (8), (10), and (13). The thrust angle at the first switching point, φ_1, is found from Eq. (12), and $\psi_1 = \psi_2 = \pi/2 - \varphi_1$. The integration constants may be computed using the expressions

$$a = \frac{m_0 - \beta t_2}{c\sin(kt_2 + \alpha)}, \qquad C_2 = -\frac{r_0}{a}$$

Then, we can find the initial primer vector magnitude as $\lambda_0 = a\sin\alpha$. Lawden's integration constants can be found from following equations:

$$P_1 = a\sin\alpha, \qquad P_2 = \frac{a\sin\gamma\sin\varphi_2}{e\sin f_2}, \qquad R_1 = -a\sin\alpha$$

$$R_2 = (1 + e\cos f_2)[P_1(1 + e\cos f_2) + a\sin\gamma\cos\varphi_2]$$

Numerical Example

The problem discussed in the preceding section is analyzed in this section using numerical values of the transfer parameters. Note that the continuity conditions at the switching points allow us to calculate the integration constants and final time to construct time histories and the transfer trajectory. The following values are used: $r_0 = 6600$ km, $\mu = 398{,}600.1445$ km^3/s^2, $k = 0.0011775$ rad/s, $m_0 = 10{,}000$ kg, $\beta = m_0/100$ kg/s, $c = 3$ km/s, $e = 1.3$, and $p = 2.3$. The variable ω can be chosen arbitrarily. When the formulas derived in the preceding section are used, the integration constants are found to be

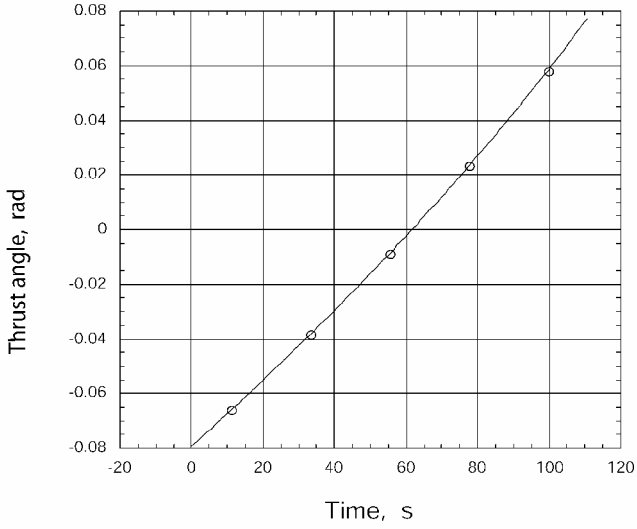

Fig. 2 Time history of φ.

$$a = -2625.9, \qquad \alpha = -1.6236$$

$$C_2 = 2.5135, \qquad \lambda_0 = 2622.2$$

The results for the switching points are given in Table 1.

To obtain a more complete qualitative picture of the transfer, the following quantities have been used: angle of asymptotes α_h, energy constant K, semimajor axes a_h, hyperbolic mean motion n_h, and dimensionless characteristic velocity of the analytical and impulsive transfer between terminal orbits, $\Delta v/v_0$. These values can easily be calculated using the formulas[13]

$$\alpha_h = \arctan\sqrt{e^2 - 1} = 39.715, \qquad K = v_p^2 - 2\mu/r_p = 18.118$$

$$r_p = p/(1 + e) = 6600.0, \qquad v_p = \sqrt{\mu/p}(1 + e) = 11.7858$$

$$a_h = p/(e^2 - 1) = \mu/K = 22000.0$$

$$n_h = \sqrt{\mu}a_h^3 = 0.00019350, \qquad v_0 = \sqrt{\mu/r_0}$$

$$\Delta v/v_0 = 0.51693, \qquad \Delta v_{\text{imp}}/v_0 = \sqrt{1 + e} - 1 = 0.51657$$

where r_p and v_p are the perigee and total velocity on the hyperbolic orbit. The difference in the dimensionless analytical and impulsive characteristic velocities is 0.00016. The errors are as follows: In the gravitational acceleration, $\epsilon_g = 1.9218e - 14$; in the dynamic model $\mathcal{O}[\Delta r(f_2)/r_0^4] = 3.2675e - 15$. The absolute error in all computations was less then 10^{-11}. The integrated trajectory results in relative differences in the magnitude of the radius vector of 0.0091. The ratio of the velocity difference to the total velocity is 0.0829. For comparison purposes, the equations of motion with MT in the Newtonian field were integrated numerically using final time and thrust direction history, which were taken from the analytical results. The time history of the thrust angle is shown in Fig. 2.

To analyze the relationships between the transfer variables and understand their behavior during the maneuver, the following sets

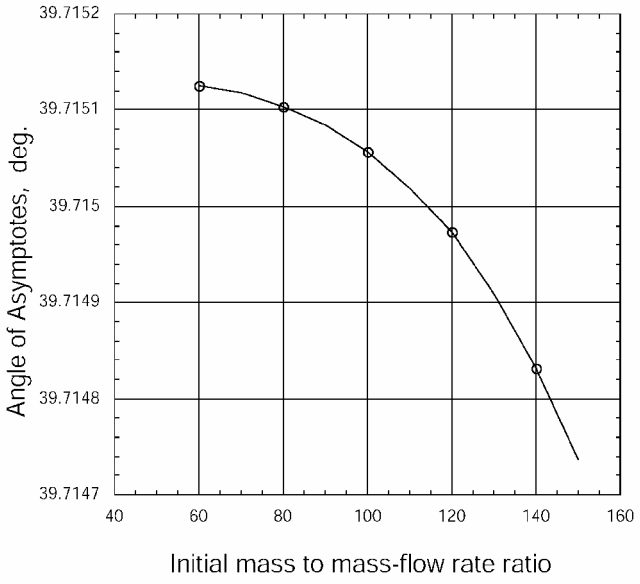

Fig. 3 Relationship between the ratio p/r_0 and angle of asymptotes: $e = 1.3$, $p/r_0 = 2.3$, and $m_0 = 10{,}000$ kg.

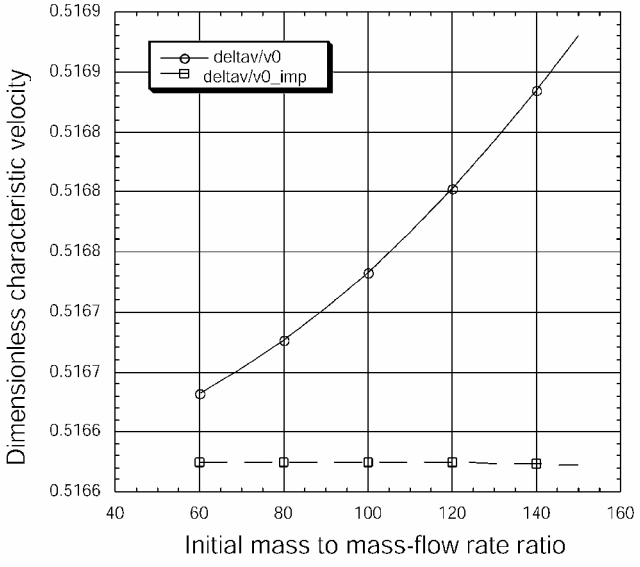

Fig. 4 Dimensionless characteristic velocities vs ratio m_0/β: $e = 1.3$, $p/r_0 = 2.3$, and $m_0 = 10{,}000$ kg.

of initial conditions have been used:

$$m_0/60 \le \beta \le m_0/150, \qquad 2.1 \le p/r_0 \le 3.8, \qquad 1 \le e \le 2.8$$

where m_0 and r_0 were fixed at the values given earlier. The computations and analysis of the results indicate that there exists an almost linear relationship of the eccentricity with the ratio p/r_0 and the energy constant. The eccentricity, energy constant, and dimensionless characteristic velocity, $\Delta v/v_0$, are less sensitive to changes in the ratio m_0/β and, except for the $\Delta v/v_0$, these parameters behave in a similar manner with respect to the ratio m_0/β at fixed eccentricity, ratio p/r_0, initial mass, and initial radius. Examples of these dependencies are shown in Fig. 3, which shows the relationship between m_0/β and the angle of asymptotes. The sensitivity of $\Delta v/v_0$ to changes in the ratio m_0/β is higher than the sensitivity of $\Delta v_{\text{imp}}/v_0$, as shown in Fig. 4. Larger values of the ratio p/r_0 result in larger values of the thrust angle. There exists only one set of eccentricity, ratio p/r_0, and flight duration for a fixed m_0/β, initial mass, and initial radius. The results indicate that the difference between $\Delta v/v_0$ and $\Delta v_{\text{imp}}/v_0$ (dimensionless characteristic velocity of the impulsive transfer) slowly increases with the flight duration, eccentricity, and ratio p/r_0 as shown in Figs. 5 and 6.

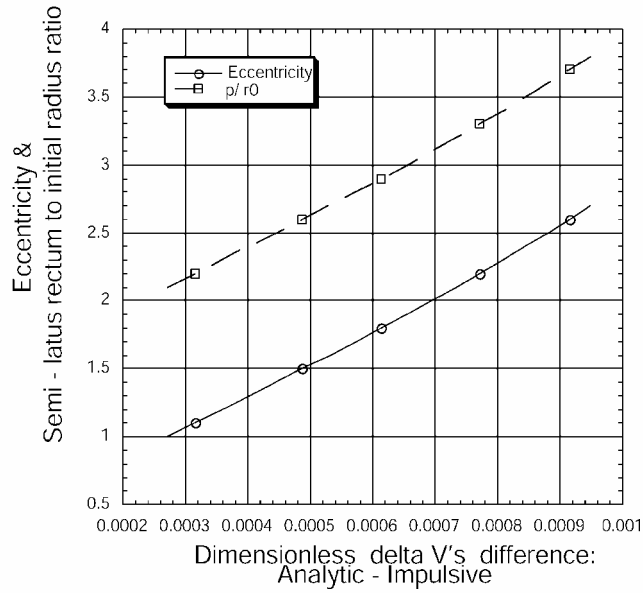

Fig. 5 Dependency between eccentriciry e, ratio p/r_0, and difference $\Delta v - \Delta v_{\text{imp}}/v_0$: $m_0 = 10{,}000$ kg and $r_0 = 6600$ km.

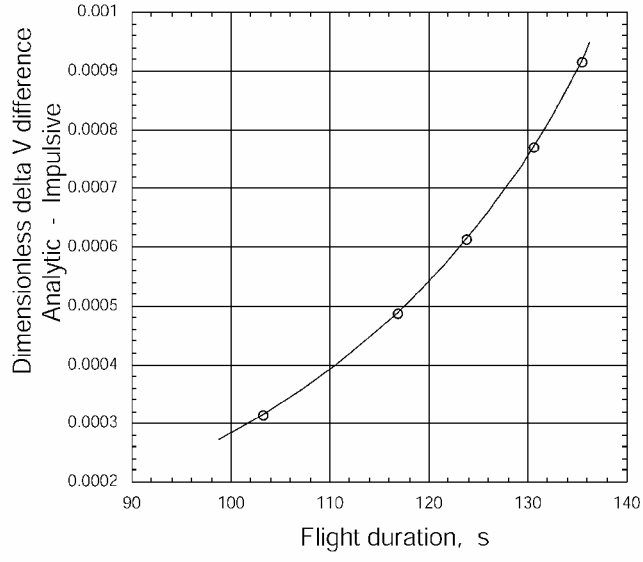

Fig. 6 Difference $\Delta v - \Delta v_{\text{imp}}/v_0$ vs flight duration: $m_0 = 10{,}000$ kg, $m_0/b = 150$, and $r_0 = 6600$ km.

The analysis confirms that the linear approximation of the gravity field can be used to analyze optimal transfer maneuvers performed within the boundaries of the aforementioned layer. Although the transfer parameters satisfy the necessary conditions of optimality, the tests for sufficiency conditions require further investigation.

Conclusions

A variational trajectory optimization problem statement that involves both LT and HT propulsion systems has been discussed. It was shown that a linear field approximation can be applied to the problem of computing MT transfers between circular and hyperbolic orbits in a Newtonian field. The corresponding analytical solutions can be used to describe all parameters of the maneuver, and impulsive transfers can be replaced by the MT arc that lies in the thin layer around the initial orbit.

References

[1]Lawden, D. F., *Optimum Trajectories for Space Navigation*, Butterworths, London, 1963. Chap. 3, pp. 54–70.

[2]Melbourne, W. G., and Sauer, C. G., "Constant-Attitude Thrust Program Optimization," *AIAA Journal*, Vol. 3, No. 8, 1965, pp. 69–74.

[3]Bishop, R. H., and Azimov, D. M., "Analytical Trajectories of an Extremal Motion with Low-Thrust Exhaust-Modulated Propulsion," *Journal of Guidance, Control, and Dynamics*, Vol. 38, No. 6, 2001, pp. 897–903.

[4]Azizov, A. G., and Korshunova, N. A., "On an Analytical Solution of the Optimum Trajectory Problem in a Gravitation Field," *Celestial Mechanics*, Vol. 38, No. 4, 1986, pp. 297–306.

[5]Azimov, D. M., and Bishop, R. H., "Extremal Rocket Motion with Maximum Thrust in a Linear Central Field," *Journal of Spacecraft and Rockets*, Vol. 38, No. 5, 2001, pp. 765–776.

[6]Tapley, B. D., "Regularization and the Computation of Optimal Trajectories," *Celestial Mechanics*, Vol. 2, No. 3, 1970, pp. 319–333.

[7]McCue, G. A., "Quazilinearization Determination of Optimum Finite-Thrust Orbital Transfers," *AIAA Journal*, Vol. 5, No. 4, 1967, pp. 755–763.

[8]Enright, P. J., and Conway, B. A., "Optimal Finite-Thrust Spacecraft Trajectories Using Collocation and Nonlinear Programming," *Journal of Guidance, Control, and Dynamics*, Vol. 14, No. 5, 1991, pp. 981–985.

[9]Kornhauser, A. L., Lion, P. M., and Hazelrigg, G. A., "An Analytic Solution for Constant-Thrust, Optimal Cost, Minimum-Propellant Space Trajectories," *AIAA Journal*, Vol. 9, No. 7, 1971, pp. 1234–1239.

[10]Novoselov, V. S., *Analytical Theory of Trajectory Optimization in the Gravitational Fields*, Leningrad State Univ. Press, Leningrad, U.S.S.R., 1972, p. 317.

[11]Azizov, A. G., and Korshunova, N. A., "On Optimal Trajectories in Gravitational Fields, Admitting Approximation by Central Linear," *Space Research*, Vol. 29, No. 4, 1991, pp. 525–531.

[12]Jezewski, D. E., "Optimal Analytic Multi-Burn Trajectories," *AIAA Journal*, Vol. 10, No. 5, 1972, pp. 680–685.

[13]Szebehely, V. G., *Adventures in Celestial Mechanics*, Univ. of Texas Press, Austin, TX, 1993, pp. 56–81.

D. L. Edwards
Associate Editor

Performance Analysis of Thermal Protection System of a Solid Rocket Nozzle

V. Jones* and K. N. Shukla†
Vikram Sarabhai Space Center, Trivandrum 695 022, India

Introduction

ABLATIVE materials are commonly used to protect the solid rocket nozzle walls exposed to high-temperature gaseous combustion products. An accurate prediction of the thermal response of these materials is essential for a nozzle thermal designer to successfully carry out the design of an optimum thermal protection system (TPS). Numerous test results on heat transfer in sea-level nozzles are available. Therefore, it is not too difficult for a nozzle thermal designer to design an optimum TPS in the case of sea-level nozzles. However, test results for high-altitude nozzles are very scarce. Consequently, a considerable degree of uncertainty exists in the estimation of wall heat flux, as well as the design of a TPS for a high-altitude rocket nozzle. The most widely used approach for computing wall heat flux in a rocket nozzle is the boundary-layer method developed by Elliott et al.[1] It is always desirable to perform a detailed study in order to supplement the existing design code and validate it with realistic test results so as to design an optimum TPS for the high-altitude rocket nozzles. The present investigation couples two different computer codes previously developed by these authors: a computational fluid dynamics (CFD) code to simulate the fluid flow inside a rocket nozzle[2] and a material thermal response code to study the in-depth response of TPS materials exposed to the hot gas flowing through the rocket nozzle.[3] These two codes are explicitly coupled through an energy balance at the common wall boundary of the nozzle. This Note presents in detail the coupling technique[4] of the two codes and compares the computed results with the test results generated in house as well as those available in the literature.

Received 13 June 2002; revision received 12 January 2003; accepted for publication 30 January 2003. Copyright © 2003 by the American Institute of Aeronautics and Astronautics, Inc. All rights reserved. Copies of this paper may be made for personal or internal use, on condition that the copier pay the $10.00 per-copy fee to the Copyright Clearance Center, Inc., 222 Rosewood Drive, Danvers, MA 01923; include the code 0022-4650/03 $10.00 in correspondence with the CCC.

*Scientist.
†Scientist. Associate Fellow AIAA.

Description of the Problem

In a solid rocket nozzle, normally the inner wall is formed with an ablative liner material such as carbon phenolic or silica phenolic, followed by its structural backup. While the rocket motor is in operation, the liner is subjected to the flow of hot gaseous combustion products, as a result heat flows from the hot gas into the liner material. The ablative liner absorbs the heat and protects the underlying structure by keeping its temperature within tolerable limits. Thus, it is essential for a nozzle thermal designer to compute accurately the heat flow rate from the hot gas into the liner material and to predict accurately the response of charring ablators exposed to the hot gas flow of combustion products.

During the days when the high-speed computing systems were yet to be invented, a closed-form equation,[5] which could be hand computed, was used for estimating nozzle wall heat flux. With the availability of high-speed computing systems, a more sophisticated solution[1] could be adopted for heat-flux computation. However, for high-altitude rocket nozzles it is always desirable to carry out a detailed study by solving Navier–Stokes (N-S) equations for computing nozzle wall heat flux and validate it with realistic test results so as to design an optimum TPS. Such a detailed analysis has now been possible, and the same has been dealt with in the following sections.

CFD in Rocket Nozzles

Jones and Shukla[2] described an analysis of the flow in a rocket nozzle and the development of the associated computer code. The steady viscous turbulent compressible flow in a converging–diverging axisymmetric nozzle is simulated through a computer code using a time-marching explicit scheme. The N-S equations governing an axisymmetric flow for the physical domain of a rocket nozzle are transformed to a rectangular computational domain with a boundary-fitted coordinate system. The effect of turbulence is incorporated in the code by using the Baldwin–Lomax model. The equations are cast into finite difference form in a variable mesh network. The functional values at the interior mesh points are computed using MacCormack's explicit predictor–corrector finite difference scheme; a two-step characteristic scheme is adopted for applying boundary conditions using two independent variables.

In addition to the computation of the usual flowfield variables such as density, pressure, velocity, temperature, etc., the momentum and energy thicknesses are also computed using the respective integrals, for the estimation of heat flux to the wall. The convective heat flux to the wall q_w is computed as follows:

$$q_w = C_h \rho U c_p (T_{\text{ad}} - T_w) \tag{1}$$

The expressions for computing other parameters such as skin friction C_f, Stanton number C_h, etc., are given by Bartz.[6] Boundary-layer interaction exponent $n = 0.1$ and C_f for film property conditions are assumed.

In-Depth Response of Wall Materials

The nozzle wall is assumed to consist of a charring ablator followed by a noncharring structural backup. An analysis and the development of a computer code to predict the in-depth response of charring ablators exposed to high-temperature environments is available elsewhere.[3] The governing mathematical equations are derived in a fixed coordinate system tied to the original surface. The adoption of